Polar Biology
https://doi.org/10.1007/s00300-023-03150-8

ORIGINAL PAPER

Temporal dynamics and environmental drivers of polar cod (*Boreogadus saida*) densities in the northeast Chukchi Sea

Silvana Gonzalez[1] · John K. Horne[1] · Seth L. Danielson[2] · Guzman Lopez[3] · Angel M. Segura[3]

Received: 21 July 2022 / Revised: 26 April 2023 / Accepted: 9 May 2023

Abstract

The Chukchi Sea pelagic ecosystem continues to undergo dramatic oceanographic changes associated with reductions in sea ice and increasing temperatures over the last decades. Impacts of these changes on polar cod (*Boreogadus saida*), an ice-associated pelagic fish that constitutes a key energetic link between lower and upper trophic levels, remain uncertain. Here, we use 4 years (2016–2019) of high-resolution acoustic and oceanographic data from the Chukchi Ecosystem Observatory to characterize temporal patterns in polar cod densities and identify its environmental drivers in years with contrasting sea ice and temperature conditions. Polar cod densities were 2–16 times greater with peaks occurring 14–60 days earlier in years with early sea ice retreat and higher water temperatures (2017 and 2019). The variance to mean relationship showed a decrease in variance for larger abundances in warmer years. Increased densities occurring earlier in the summer are attributed to a combination of earlier and increased transport of polar cod eggs and larvae from spawning areas, enhanced local primary and secondary production, and increased growth rates of fish due to higher temperatures. Earlier sea ice retreat and increases in temperature could temporarily benefit polar cod production in the NE Chukchi Sea but potential changes in prey quality, mismatch between polar cod and its prey, and increased competition with boreal fish species could have detrimental effects on polar cod populations with further warming. Such effects on polar cod populations could propagate through pelagic Arctic food webs impacting higher trophic levels and human communities.

Keywords Acoustic backscatter · Polar cod · Chukchi Sea · Arctic pelagic ecosystem

Introduction

The Chukchi Sea is a highly productive environment and represents a major gateway to the Arctic. Pacific water entering the Chukchi Sea shelf through the Bering Strait is rich in nutrients, phytoplankton, and zooplankton and a source of nutrients, heat, and freshwater. The Chukchi Sea environment is changing rapidly (Stroeve and Notz 2018; Danielson et al. 2020b; Timmermans and Labe 2020). Increases in water temperature over the last century that have intensified since the 1990s (Steele et al. 2008; Danielson et al. 2020a) are coupled with drastic reductions in the duration of the sea ice covered season (Serreze et al. 2016), in sea ice and snow cover thickness (Kwok 2018), and in multiyear ice (Wu and Wang 2018). Changes in sea ice affect the entire underwater environment as it modulates underwater light irradiance, sea surface temperature, stratification/mixing of the water column, and subsequent nutrient replenishment (Mundy et al. 2005; Hill et al. 2018b). These changes have promoted a likely increase in primary production (e.g. Arrigo and van Dijken 2015; Lewis et al. 2020), a shift towards smaller phytoplankton and zooplankton species (e.g. Hop et al. 2006; Li et al. 2009; Møller and Nielsen 2020), changes in species phenology (e.g. Søreide et al. 2010; Ji et al. 2013; Ardyna and Arrigo 2020), and northward expansion of boreal fish and zooplankton species distributions (e.g. Fossheim et al. 2015; Polyakov et al. 2020).

Continued biological responses to large and rapid changes in the physical environment in the Chukchi Sea remain

✉ Silvana Gonzalez
silgonz@uw.edu

[1] School of Aquatic and Fishery Sciences, University of Washington, BOX 355020, Seattle, WA 98195, USA

[2] College of Fisheries and Ocean Sciences, University of Alaska Fairbanks, Fairbanks, AK 99775, USA

[3] Departamento de Modelización Estadística de Datos E Inteligencia Artificial (MEDIA), Centro Universitario Regional Este, Universidad de La República, 27000 Rocha, Uruguay

Published online: 17 May 2023

poorly documented and uncertain (Grebmeier 2012; Post et al. 2013; Assmy et al. 2017; Drinkwater et al. 2018). This uncertainty is attributed to the net effects of spatial and temporal change from multiple factors and limited, long term synchronous measurements of biological and physical environmental components. A better understanding of biological responses to further changes in Arctic pelagic ecosystems requires identification of environmental factors associated with existing biological patterns, and the characterization (i.e. strength and shape) of those associations using concurrent physical and biological data across multiple years.

Polar cod (*Boreogadus saida*) is the most abundant fish species in the NE Chukchi Sea and has been identified as a species of potential commercial importance in the Arctic Fishery Management Plan (NPFMC 2009). This dominant species constitutes a key link between trophic levels within the Arctic ecosystem (Welch et al. 1992; Whitehouse et al. 2014) being an important prey for birds, seals and whales (Bluhm and Gradinger 2008; Divoky et al. 2015; Harwood et al. 2015). Polar cod is often associated with sea ice, where it feeds and spawns (Graham and Hop 1995; Bouchard and Fortier 2011). Therefore, changes in sea ice concentrations and timing have both direct and indirect effects on temporal patterns of polar cod densities that in turn can affect the flow of energy in the Arctic food web and the services it provides to northern human communities (Darnis et al. 2012). Increased water temperature due to earlier annual sea ice retreat and increased inflow of warm Pacific waters into the Chukchi Sea have been hypothesized to enhance growth and transport of age-0 polar cod from spawning sites located in the south (Levine et al. 2021). However, changes in polar cod zooplankton prey quality and potential increases in predation and competition with boreal fish species could have detrimental effects on polar cod populations (Marsh and Mueter 2019). At this time, overall effects of environmental changes on polar cod remain uncertain.

Four years of continuous, high-resolution biological and physical data streams from the Chukchi Ecosystem Observatory (CEO) are available to: (1) characterize temporal patterns in polar cod densities, and (2) identify and quantify relationships between polar cod densities and environmental factors in years with contrasting sea ice and water temperature. Understanding bio-physical patterns in years with different sea ice conditions can help elucidate potential biological responses to further changes in the environment.

Methods

Study area

The CEO is located on the NE Chukchi Sea shelf between Hanna Shoal and Barrow Canyon (71° 35.976′ N, 161° 31.621′ W) at 46 m depth (Fig. 1). Located on a documented hotspot of benthic biomass (Grebmeier et al. 2015), the CEO area attracts populations of upper trophic level consumers (Jay et al. 2012; Hannay et al. 2013). The CEO seascape varies seasonally with a late fall and winter homogeneous water column with thickening sea ice and light-limited primary production (Weingartner et al. 2005b). Spring is characterized by diatoms and sea ice algae blooms triggered by the return of light (Gradinger 2009; Arrigo et al. 2014). When sea ice starts to melt after May, a stratified, warmer, nutrient-rich water column triggers massive phytoplankton blooms under the ice (Arrigo et al. 2012) that continue through the summer (Hill et al. 2018a). In the fall, the intensification of winds and diminishing solar input allows the water column to re-homogenize and surface waters are replenished with nutrients that support fall phytoplankton blooms until sunlight fades.

The Chukchi Sea continental shelf waters are fed by northward-flowing waters from the North Pacific carrying heat, freshwater, and nutrients through the Bering Strait (Fig. 1). This transport is driven by a seasonally fluctuating Pacific–Arctic pressure head (Stigebrandt 1984; Aagaard et al. 2006) that transmits 1.0–1.2 Sv during summer and 0.5–0.6 Sv during winter months (Woodgate et al. 2005a). Water flowing through the Bering Strait is routed across the Chukchi Shelf along three main pathways: Herald Canyon in the west, Barrow Canyon in the east and the Central Channel across the mid-shelf, although wind-driven and other fluctuations episodically modify or even reverse these flows (Weingartner et al. 2005a; Woodgate et al. 2005; Danielson et al. 2014).

Environmental data

A set of environmental data collected at the CEO (https://aoos.org/project-page/ecosystems/chukchi-ecosystem-observatory/) during the study period (2016–2019) was supplemented with data from other sources for this study. Midwater measurements of salinity, temperature, photosynthetically active radiation (PAR), fluorescence, and nitrate concentration were collected hourly at the CEO using a Sea-Bird Scientific SBE-16 SeaCat and a Satlantic SUNA sensor deployed at 28–33 m depth. Bottom temperature and salinity measurements were collected hourly using a Sea-Bird SBE-37 MicroCat located at a depth of 43 m (seafloor depth of 46 m).

In situ fluorescence concentration measurements (a proxy for chlorophyll *a* concentration) were not available for the August 15th 2017–August 5th 2018 period and were predicted using the auto-sklearn machine learning tool kit (Feurer et al. 2015). The automatic machine learning framework takes a Bayesian optimization algorithm to automate feature engineering, regressor selection, and

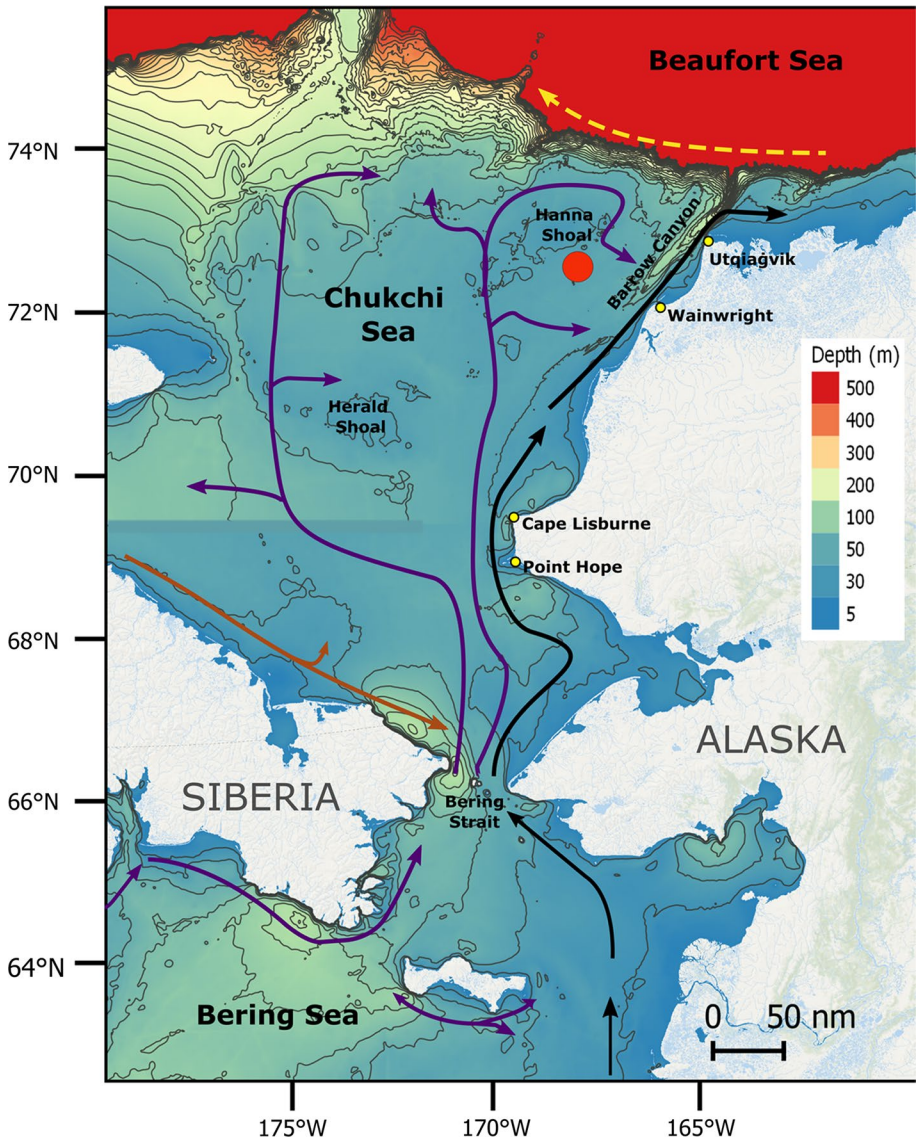

Fig. 1 Study region map including bathymetry and main flow pathways. The yellow arrow represents the Beaufort Gyre, black arrows represent the Alaskan Coastal Current, the brown arrow represents the Siberian Coastal Current, and purple arrows represent pathways of Bering Shelf, Anadyr, and Chukchi shelf waters. The red circle indicates the location of the Chukchi Ecosystem Observatory. Scale in nautical miles (nm)

hyper-parameter adjustment (Feurer et al. 2015). This method fits a statistical model to observed in situ fluorescence based on daily averages of the variables described above, and then applies model-based predictions to estimate missing fluorescence values. Daily measurements of chlorophyll *a* from the MODIS sensor on the NASA Aqua satellite (https://polarwatch.noaa.gov/) were also included as a predictor variable in the models. A 10-fold cross validation data resampling method was used to split the dataset into training and testing samples. The coefficient of determination (R^2) between observed and predicted fluorescence values was used as the optimization metric during training. Accuracy of predictions was evaluated using R^2, mean absolute percentage error, and root mean squared error (RMSE).

Satellite-based, sea ice concentration (%) daily average data were downloaded from the National Snow and Ice Data Center (NSIDC) archive (http://nsidc.org/data/seaice/pm.html#pm_seaice_conc) (Maslanik and Stroeve 1999). The onset of sea ice retreat and advance, defined as the first day with sea ice concentration less than 30% and exceeding 30%, were identified for each year (Serreze et al. 2016). Daily sunrise and sunset times at the CEO were obtained using the 'sunriset' function of the R package *maptools* (v. 0.9-9, Bivand & Lewin-Koh 2019) and used to calculate daylength, a proxy of light irradiance throughout the year. Daily air temperatures recorded at the nearby coastal city of Utqiaġvik were obtained from the U.S. climate data website (https://www.usclimatedata.com/climate/barrow/alaska/united-states/usak0025). Hourly wind speed data for the CEO location were obtained from the Copernicus Climate Change Service ERA5 dataset (Hersbach et al. 2018).

Acoustic data acquisition, processing, and classification

Four years (2016–2019) of active acoustic data were used to characterize temporal patterns in polar cod densities in the Chukchi Sea (Fig. 1). Acoustic backscatter data, a proxy for fish density, were collected using an ASL Acoustic Zooplankton Fish Profiler (http://www.aslenv.com/AZFP.html), deployed at 28–35 m depth (depending on year), looking upwards, and operating at 36, 125, 200, and 455 kHz.

Acoustic backscatter corresponding to fish was discriminated from other sources of backscatter using differences in mean volume backscattering strength (MVBS; Madureira et al. 1993; Kang et al. 2002; Korneliussen and Ona 2003) between 125 and 38 kHz data (ΔMVBS125-38 kHz). Fish Sv values were integrated into hourly averages from January 1, 2016 to December 31, 2019. A detailed description of the CEO acoustic data collection and processing can be found in (Gonzalez et al. 2021).

Although no direct fish sampling was conducted in association with acoustic measurements, we can rely on catch data from fisheries surveys carried out in the NE Chukchi Sea to attribute most of the observed fish backscatter to polar cod. Polar cod accounted for 81–90% of total fish biomass and abundance from bottom (Barber et al. 1997; Goddard et al. 2014; Sigler et al. 2017; Logerwell et al. 2018) and pelagic (Lowry and Frost 1981; De Robertis et al. 2017) trawl surveys conducted from spring through autumn, ice-free seasons. Polar cod constituted the majority of fish biomass (63–99%) and abundance (93–99%) in sample catches from four midwater trawls conducted on Hanna Shoal in close proximity to the CEO in summer of 2017 (Levine and De Robertis pers. comm). Other species caught near Hanna Shoal included capelin (*Mallotus villosus*), *Lumpenus* sp., staghorn sculpin (*Gymnocanthus tricuspis*), and Liparidae snailfish. As further support of this backscatter classification, age-0 (i.e. < 12 months old) polar cod was the dominant contributor to 38 kHz backscatter in the northern region of the Chukchi Sea in acoustic-trawl surveys conducted in 2012 and 2013 as part of the Arctic Ecosystem integrated survey (De Robertis et al. 2017) and constituted > 85% of the catch per unit effort in a 2019 survey in the Chukchi Sea (Levine et al. 2021).

Data analysis

Characterization of temporal patterns in polar cod backscatter

Ecosystems have complex dynamics that result from the combined effects of population dynamics, environmental variability, and species interactions. Macroscopic patterns, detected using power laws, can provide general descriptions of a system without including detailed information on interacting agents (Maurer 1999; Cohen et al. 2012; Segura et al. 2021). These macroscopic patterns characterize dynamical and static patterns for comparison among populations, ecosystems, or environmental conditions.

One effective way to summarize temporal patterns of a species is using Taylor's power law (TPL). TPL states that the spatial or temporal variance (V) in population abundance (N) is related to the mean (M) population abundance: $V[N] = aM[N]^b$ (Taylor 1961), with the coefficient a and the scaling exponent b that approximates a value of 2. Conceptually, the scaling component b captures the level of aggregation between individuals in a population, while the coefficient a is considered an artifact of sampling methodology (Taylor 1961). When mean–variance pairs are estimated from abundances measured through time at the same location, fluctuations in the temporal aggregation of a population are described. The scaling exponent has been used as an ecological metric to compare fish populations between regions of contrasting environmental characteristics (e.g. Mellin et al. 2010; Cobain et al. 2019), at varying levels of fishing pressure (e.g. Cohen et al. 2012; Fujiwara and Cohen 2015; Kuo et al. 2016; Segura et al. 2021), and between fish species with different life histories (e.g. Kuo et al. 2016).

Daily mean and variance in backscattering strength from polar cod were calculated from hourly values of the volume backscatter coefficient [sv: units: m^{-1}; linear form of Sv (dB)]. Days with less than 5 backscatter observations were excluded from the analysis to avoid bias in variance estimates. The TPL exponent and coefficient were estimated from the linear relationship of the base 10 logarithms of the sample's variance and mean described by:

$$\log_{10}\left(V\left[s_{\mathrm{V}}\right]\right) = \log_{10}(a) + b\log_{10}\left(M\left[s_{\mathrm{V}}\right]\right) + \varepsilon,$$

where ε is the residual error. TPL exponents and coefficients estimated using ordinary least squares linear relationships were compared among years. The null expectation for TPL for temporal variation is that the slope of the log-variance versus log-mean plot equals 2. Confidence intervals (95% level) were used to contrast estimated scaling exponents against the null hypothesis and to compare the exponents among years.

Environmental drivers of polar cod densities

To identify associations between polar cod densities and environmental variables at the CEO we used Generalized Additive Models (GAMs). GAMs are nonlinear regression models in which relationships between the response variable and predictor variables are modeled using nonparametric smooth functions (Hastie and Tibshirani 1990;

Wood 2004, 2017). GAMs represent an effective modeling approach for assessing responses of fish communities to environmental factors (e.g. Sigler et al. 2015; Logerwell et al. 2018; Forster et al. 2020). The advantage of this method is that it is not necessary to specify the relationship between the variables a priori as these are determined from the data. Specifically, given a response variable y and a set of m predictor variables x (covariates), the relationship between the two is established by:

$$y_i = \alpha + \sum_{j=1}^{m} s_j(x_{ji}) + e_i.$$

The error term, e_i is generally assumed to be independent and identically distributed with zero mean and common variance. The s_j are smooth nonparametric functions estimated using thin plate regression splines (Wood 2017). Smoothing parameters were selected using restricted maximum likelihood (REML) which penalizes overfitting more than other methods (Wood 2011).

Daily averages of MVBS attributed to polar cod were used as a response variable. Days with no backscatter (7% of measurements) were excluded so fitted GAMs describe the densities of polar cod when present. Daily averages of midwater and bottom temperature and salinity, sea ice concentration, number of days after sea ice retreat, air temperature, chlorophyll *a* concentration, PAR, nitrate concentration, wind speed, and daylength were included as covariates in candidate models. Year was included as a factor in all models. Time series of environmental covariates included in candidate GAMs are included in Online Resource 1. Collinearity among covariates was identified from the variance inflation factor (VIF) using a value of less than 5 as a cutoff for inclusion of covariates in the same candidate model (Zuur et al. 2009).

GAMs were fitted using the *mgcv* (version 1.8-38; Wood 2017) package in R with a Gaussian distribution and identity link function. To account for autocorrelation in the time series, an AR(1) (i.e. autocorrelation of order one) term was included in all candidate models. The model with the lowest Akaike information criterion (AIC) was selected. Residuals from each model were visually compared to the normal distribution using quantile–quantile plots. Autocorrelation functions (ACF), and partial ACFs (PACF) were used to check for remaining autocorrelation within the residuals.

Results

Temporal patterns in environmental variables and polar cod backscatter

Our study spanned years with highest temperatures and lowest sea ice conditions on record but strong differences in temperature and sea ice conditions among sample years were observed. Years 2016 and 2018 (hereafter "cold" years) were characterized by later sea ice retreat, earlier advance, greater sea ice concentration, and lower water temperatures than 2017 and 2019 (hereafter "warm" years). Sea ice retreat occurred on July 13th 2016, June 3rd 2017, July 14th 2018, and May 12th 2019 (Fig. 2a). Sea ice advance occurred on November 21st 2016, December 5th 2017, November 23rd 2018, and December 7th 2019 (Fig. 2a). This resulted in longer open water periods (i.e. period between sea ice retreat and advance dates) in 2017 (185 days) and 2019 (209 days) than in 2016 (131 days) and 2018 (132 days). We emphasize that years labeled here as "cold" and "warm"

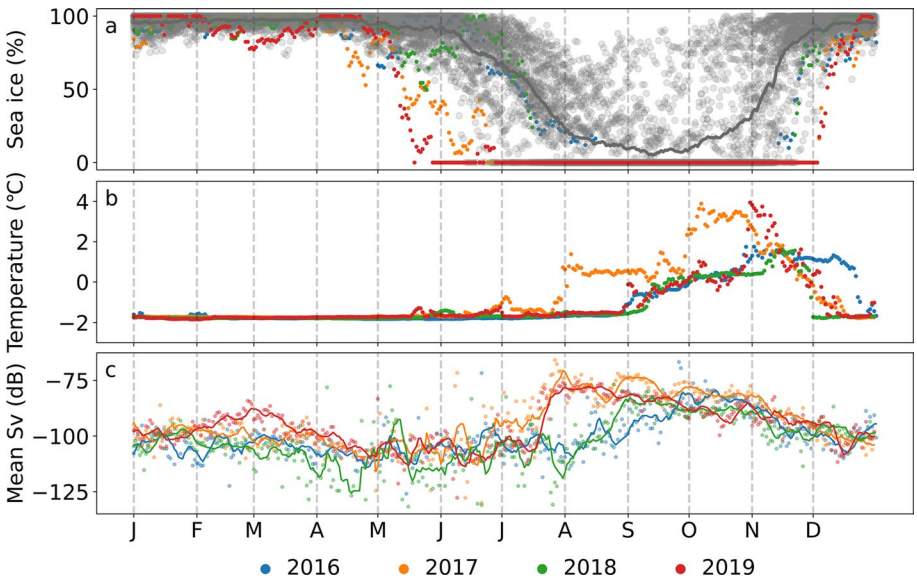

Fig. 2 Biological and physical patterns at the Chukchi Ecosystem Observatory. **a** Daily sea ice concentration from satellite data. Grey circles represent values from 1978 to 2015 and the grey line represents the average sea ice concentration for that period. **b** Daily averages of in situ measurements of midwater temperature. **c** Daily mean backscattering strength (mean Sv) values corresponding to polar cod. Lines represent weekly moving averages

were all characterized by highest temperatures and lowest sea ice conditions on record. Retreat and advance dates in 2016–2019 were up to 2 months earlier than the historic mean retreat date (July 27th) and about 1 month later than the historic advance date (October 31st) resulting in open water seasons longer than the historic average of 96 days for all years. Annual average sea ice concentrations were lower in 2017 (43%) and 2019 (40%) than in 2016 (58%) and 2018 (57%). These annual average sea ice concentrations were below the historic (1975–2015) average (67%) in all sample years.

Maximum midwater temperatures recorded at the CEO were greater in 2017 (3.87 °C) and 2019 (3.83 °C) than in 2016 (2.11 °C) and 2018 (1.31 °C) (Fig. 2b). Midwater temperature peaks occurred on October 28th in 2016, October 6th in 2017, November 15th in 2018, and on November 1st in 2019 (Fig. 2b). Average midwater temperatures were − 1.04 °C in 2016, − 0.53 °C in 2017, − 1.31 °C in 2018, and − 1.02 °C in 2019. Midwater temperatures in 2017 and 2019 were higher than in 2016 and 2018 during late spring–early summer (June–mid July) and during Autumn (late October–mid November) (Fig. 2b).

Peaks in fish acoustic backscatter attributed to polar cod had higher amplitude and occurred earlier in the summer in "warm" compared to "cold" years (Fig. 2c). Peak Sv values of − 80.97 dB (9/29/2016), − 70.60 (7/31/2017), − 82.81 dB (9/2/2018), and − 77.80 dB (8/19/2019) were observed in the 7-day smoothed series (Fig. 2c). In "warm" years, peak values were ~ 3–12 dB greater than in "cold" years corresponding to ~ 2–16 times more fish in years with earlier sea ice retreat and higher water temperatures. Peaks in Sv values occurred 14–60 days earlier in "warm" than "cold" years. Peaks in Sv occurred 78 days after sea ice retreat in 2016, 58 days in 2017, 50 days in 2018, and 99 days in 2019.

Highest fish acoustic backscatter values were associated with Modified Winter Water (MWW), cool Shelf Water (cSW), and warm Shelf Water (wSW) with temperatures above − 1 °C and salinities of 31.5–32.5 (Fig. 3). wSW was only present in 2017 and 2019 when overall temperatures were higher in the study area (Fig. 3). Days with an empty water column only occurred in presence of Winter Water (WW, Fig. 3).

Medians of the non-zero backscatter values were greater (Kruskal–Wallis $p < 0.05$) in "warm" years (− 95.10 dB in 2017 and − 95.31 dB in 2019) than in "cold" years (− 101.47 dB in 2016 and − 101.10 dB in 2018) (Fig. 4). Most frequent backscatter values were ~ − 100 dB all years but a second mode at relatively high backscatter values

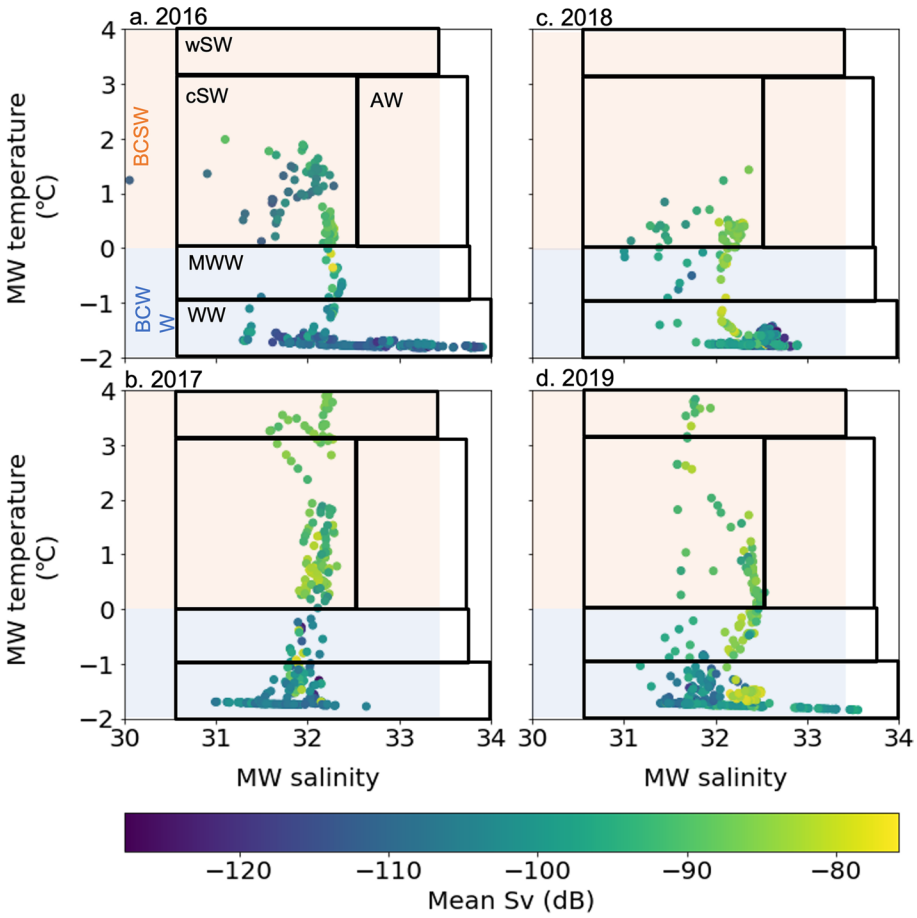

Fig. 3 Daily averages of midwater temperature and salinity measured at 33 m depth at the Chukchi Ecosystem Observatory during 2016–2019. Color bar represents mean volume backscattering strength (mean Sv, dB) corresponding to fish. Classification of water masses was based on Danielson et al. (2017, 2020). Abbreviations include: *MWW* Modified Winter Water, *WW* Winter Water, *wSW* warm Shelf Water, *cSW* cool Shelf Water, *AW* Anadyr Water. The orange and blue areas represent Bering–Chukchi Summer Water (BCSW) and Bering–Chukchi Winter Water (BCWW), respectively

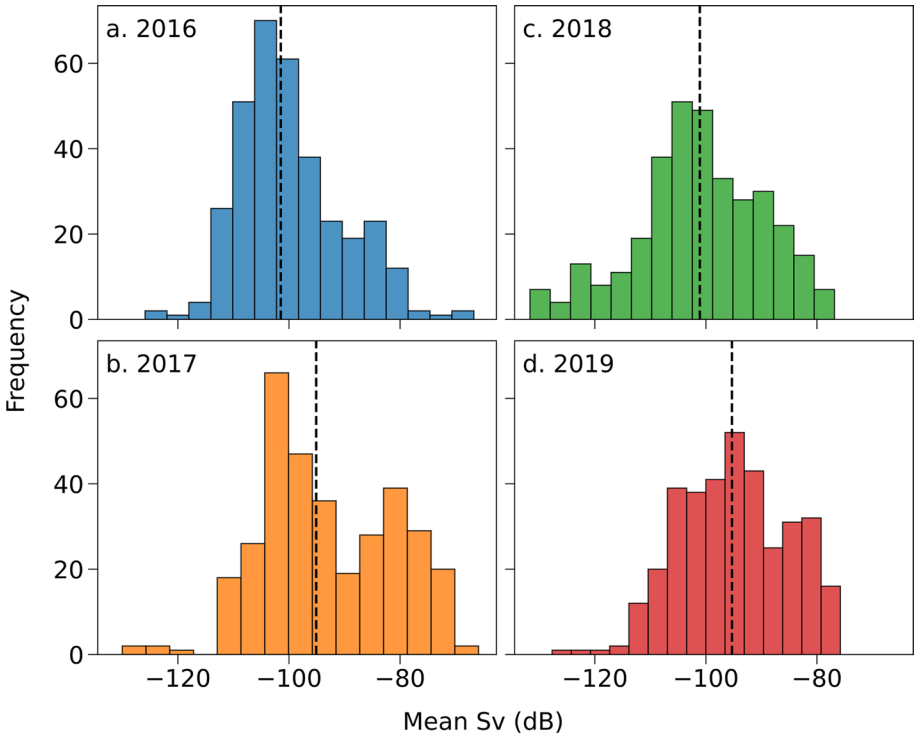

Fig. 4 Distribution of daily averages of hourly mean backscattering strength (mean Sv) values corresponding to polar cod (*Boreogadus saida*) for 2016–2019. The dashed line indicates the median

(greater than ~ −85 dB) was observed during "warm" years (Fig. 4). During "cold" years, the percentages of hours with no backscatter were greater (69% in 2016 and 63% in 2018) than in "warm" years (51% in 2017 and 43% in 2019).

Peaks in variance occurred 27–56 days earlier in "warm" years than in "cold" years (Fig. 5). Highest variances were observed during autumn months in 2016 (October 7th) and 2018 (September 11th) and in the summer in 2017 (August 12th) and 2019 (August 14th). Overall, variability was highest in 2017 (−153.40 dB) followed by 2016 (−157.16 dB), 2019 (−167.03 dB), and 2018 (−172.64 dB). In "warm" years, variance was higher than in "cold" years during July–September and mid-January–April.

Significant relationships between log-variance and log-mean sv were observed all years ($p < 0.05$) with coefficients of determination (R^2) greater than 0.94 (Fig. 6). Variance increased faster (i.e. slope b significantly greater) in 2016 ($b = 2.36$ [95% CI 2.24, 2.48]) and 2018 ($b = 2.16$ [2.07, 2.25]) than in 2017 ($b = 1.79$ [1.73, 1.86]) and 2019 ($b = 1.93$ [1.87, 1.98]). The scaling exponent b was significantly greater than the theoretical value of 2 in "cold" years, and significantly below 2 in "warm" years (Fig. 6). These observations suggest that overall, polar cod at the CEO experiences greater temporal fluctuations (i.e. shorter persistence time) in density during "cold" years than in "warm" years. Regression lines intersect each other at $\log_{10}M(\text{sv}) \sim -9$ dB (corresponding to a mean Sv of −90 dB) with "warm" years exhibiting higher variability at low fish densities and lower variability at relatively high densities than "cold" years.

Average chlorophyll *a* concentrations from in situ fluorescence measurements were higher in 2017 (1.04 mg m^{-3}) and 2019 (1.16 mg m^{-3}) compared to 2016 (0.64 mg m^{-3})

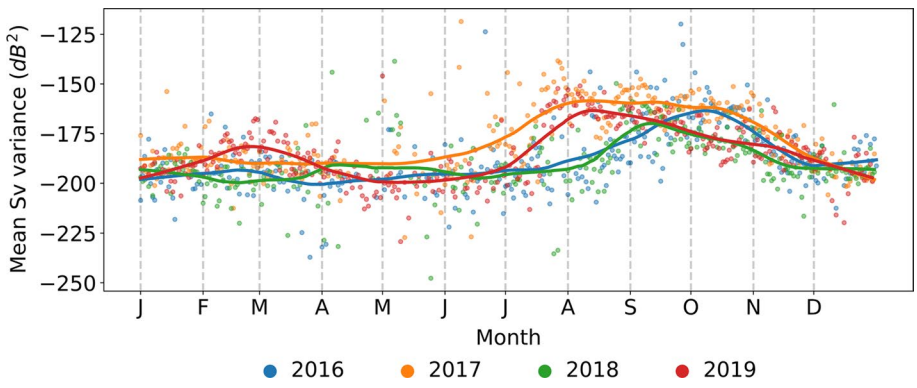

Fig. 5 Variance calculated over a 1-day period from hourly mean backscattering strength (mean Sv) values corresponding to polar cod (*Boreogadus saida*). Lines represent LOWESS smoothing with window size = 0.2 for each year

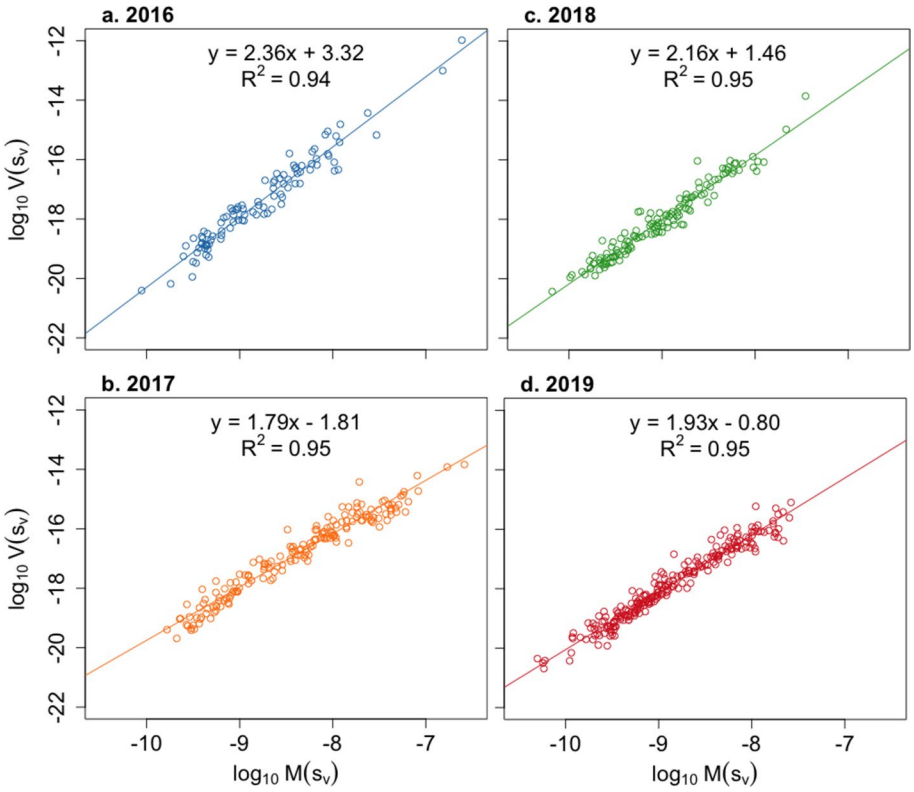

Fig. 6 Relationship between daily averages (*M*) and variance (*V*) calculated from hourly backscattering values corresponding to polar cod (*Boreogadus saida*) at the Chukchi Ecosystem Observatory. The quantity sv is the volume backscatter coefficient [linear form of volume integrated energy Sv (dB)], units: m^{-1}

and 2018 (0.82 mg m^{-3}) (Fig. 7a). Peaks in chlorophyll *a* occurred earlier and persisted over longer periods in "warm" years than in "cold" years (Fig. 7a). Multiple chlorophyll *a* peaks were observed from mid-May to August/September in 2017/2019 with the first peak observed in early June (8th–10th), 5–29 days after sea ice retreat (Fig. 7a). This indicates that an earlier sea ice retreat triggers and earlier phytoplankton blooms but not before June. In "cold" years highest chlorophyll *a* concentrations were observed from mid-June/July to mid-August in 2016/2018 with peak concentrations occurring once there was no sea ice in the area (Fig. 7a). Interannual variations in nutrient concentrations and PAR are shown in Online Resource 2.

Zooplankton backscatter was higher in spring and summer in "warm" than in "cold" years (Fig. 7b). In 2019 when sea ice retreat occurred in May, zooplankton densities were lower than in 2017, when sea ice retreat was in June (Fig. 7b). The medians of zooplankton backscatter distributions were – 89.64 dB (2016) and – 83.74 dB (2018) in "cold" years, and – 77.13 dB (2017) and – 82.42 dB (2019) in "warm" years, with 2019 being higher but more similar to the median in "cold" years.

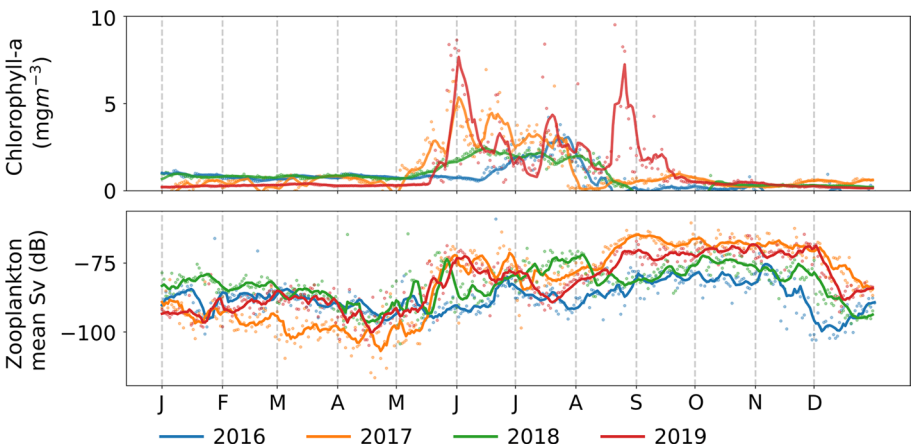

Fig. 7 Daily averages of **a** in situ midwater (33 m depth) measurements of chlorophyll *a* fluorescence, and **b** mean volume backscattering strength (Mean Sv) corresponding to zooplankton at the Chukchi Ecosystem Observatory during 2016–2019. Lines represent a 7-day moving average

Environmental drivers of polar cod densities

Polar cod acoustic backscatter was predominantly associated with days after sea ice retreat and, to a lesser extent, with bottom temperature, midwater salinity, PAR, daylength, and the cube of wind speed (Fig. 8; Table 1). The resulting GAM had an R^2 of 0.63 and the autocorrelation of the residuals was reduced significantly by the inclusion of an autoregressive lag 1 process in the model (Online Resource 3). The association between polar cod and sea ice was positive from ~ 30 days before until ~ 100 days after sea ice retreat when fish densities started to decrease (Fig. 8a). The relationship between polar cod densities and bottom temperature was linear and slightly positive (Fig. 8b). Highest backscatter values were observed at salinities above 32, cubed wind speed of less than 1000 (m^3 s^{-3}), PAR values of 5–7 molμ photons m^{-2} s^{-1}, and daylengths of 10–20 h (Fig. 8c–f). Parametric coefficients (i.e. intercepts) significantly differed

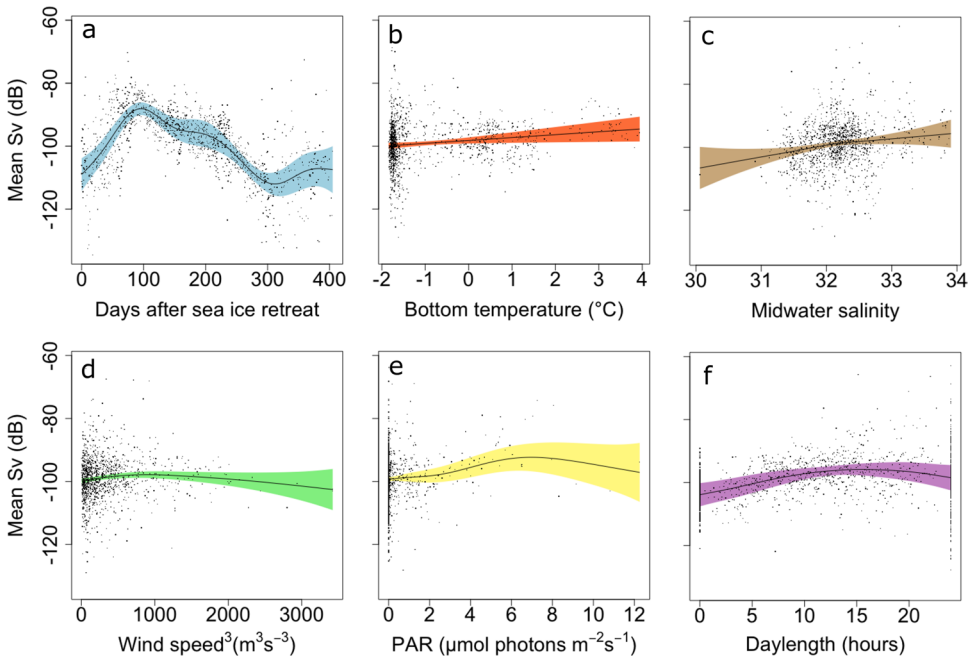

Fig. 8 Partial effects of covariates included in the polar cod (*Boreogadus saida*) backscatter Generalized Additive Model. Shaded areas indicate 95% confidence intervals. Points correspond to residual values

Table 1 Results of Generalized Additive Models for polar cod (*Boreogadus saida*) backscatter at the Chukchi Ecosystem Observatory

Model	AIC	ΔAIC
Mw. temp. + ice retreat + mw. salinity + ws^3 + PAR + daylength	8791.14	0
B. temp. + ice retreat + mw. salinity + chl-a + ws^3 + PAR + daylength	8794.258	3.118
B. temp. + ice retreat + mw. salinity + chl-a + ws^3 + PAR + daylength + NO_3	8796.438	5.298
B. temp. + ice retreat + mw. salinity + chl-a + ws^3 + PAR	8809.9	18.76
Air temp. + mw. salinity + sea ice % + NO_3 + daylength + PAR + ws	8862.274	71.134
Mw. salinity + sea ice % + NO_3 + daylength + PAR + ws	8862.94	71.8
Mw. temp. + mw. salinity + sea ice % + NO_3 + daylength + PAR + ws	8863.786	72.646
Mw. temp. + mw. salinity + sea ice % + NO_3 + daylength + PAR + chl-a + ws	8866.059	74.919
B. temp. + mw. salinity + sea ice % + NO_3 + daylength + PAR + chl-a + ws	8866.621	75.481
B. temp. + mw. salinity + sea ice % + NO_3 + daylength + PAR + chl-a	8869.056	77.916
B. temp. + sea ice % + mw. salinity + chl-a + ws^3 + PAR	8891.294	100.154
B. temp. + sea ice % + mw. salinity + chl-a + ws^3	8896.673	105.533
B. temp. + sea ice % + mw. salinity + chl-a	8898.18	107.04
B. temp. + sea ice %	8910.002	118.862
B. temp. + sea ice % + b. salinity	8912.937	121.797

Mw. temp. midwater temperature, *mw. salinity* midwater salinity, *ice retreat* days after sea ice retreat, *ws* wind speed, *PAR* photosynthetically active radiation, *chl-a* chlorophyll *a* concentration, *sea ice %* sea ice concentration, *NO_3* nitrate concentration, *b. temp* bottom temperature, *b. salinity* bottom salinity

between "cold" (2016 and 2018) and "warm" years (2017 and 2019) (Online Resource 3).

Discussion

Temporal patterns in environmental variables and fish backscatter

Our data spanned years with contrasting sea ice and water temperature conditions that were associated with dramatic differences in fish density and phenology in the NE Chukchi Sea. Higher peaks in fish density and variance occurring earlier in the summer during years with early sea ice retreat and high temperatures are attributed to a combination of (1) earlier and increased transport of age-0 polar cod from spawning areas; (2) increased prey availability due to increased local primary production followed by increased secondary production due to an earlier sea ice retreat; and (3) increased growth rates of fish due to higher temperatures. A summary of temporal patterns of polar cod and relevant environmental variables is presented in Fig. 9.

The two sets of sea ice and water temperature characteristics observed in 2016/2018 and 2017/2019 are attributed to contrasting northward heat fluxes through the Bering Strait. Sea ice retreat and advance dates in the Chukchi Sea are associated in part with the mean northward transport of relatively warm Pacific waters through the Bering Strait during April–June and during the summer months, respectively (Serreze et al. 2019). In 2017, moorings in the Bering Strait recorded one of the highest heat inflows in the last three decades (Woodgate and Peralta-Ferriz 2021). This high heat inflow resulted from high water transport (~ 1.2 Sv) and temperatures of 4 °C as early as June, ~ 0.2 Sv and 2° higher than those recorded in 2016, 2018, and the climatological average for the same month (Woodgate and Peralta-Ferriz 2021). This upstream observation is consistent with the resulting early sea ice retreat and the extended open water season in the Chukchi Sea during 2017 and probably 2019, the 2 years with lowest sea ice concentrations on record in the area (Serreze et al. 2019). Greater northward heat fluxes through the Bering Strait and longer exposure to solar radiation due to earlier retreat and later advance of sea ice are also consistent with the higher temperatures (1.7–2.7 °C more) recorded at the CEO in 2017 and 2019 compared to 2016 and 2018.

Polar cod aggregations found in the NE Chukchi Shelf are mainly comprised of small, age-0 individuals possibly advected from spawning areas located further South (De Robertis et al. 2017; Forster et al. 2020; Levine et al. 2021). Polar cod potential spawning areas have been proposed near St. Lawrence Island in the northern Bering Sea, east of the Chukotka Peninsula in western Bering Strait, and the Beaufort Sea (Kono et al. 2016; Vestfals et al. 2019; Mueter et al. 2020). Polar cod are known to spawn under sea ice during autumn and winter (Graham and Hop 1995), and early stages of polar cod are believed to be advected into the NE Chukchi Shelf by ocean currents in the spring (Forster et al. 2020; Levine et al. 2021). Higher fish densities occurring earlier in the summer at the CEO were associated with elevated northward water transport from the northern Bering and southern Chukchi Seas into the northern Chukchi Sea in 2017 and 2019. Additionally, highest backscatter values were observed in BCSW that flows north into the Chukchi Sea from the northern Bering Sea shelf (Danielson et al. 2017). In combination, these water fluxes provide further support for the hypothesis that age-0 polar cod are advected from the South by prevailing northward currents in the spring, rather than potential spawning sites in the Beaufort Sea.

Earlier sea ice retreat and warmer waters could have enhanced polar cod survival by favoring early hatchers, which resulted in the high densities observed at the CEO in 2017 and 2019. Polar cod larvae hatch under sea ice from January to July and develop in surface waters over spring and summer (Bouchard and Fortier 2011; Geoffroy et al. 2016). In general, early hatchers (i.e. those hatching during winter/early spring) have the advantage of an extended

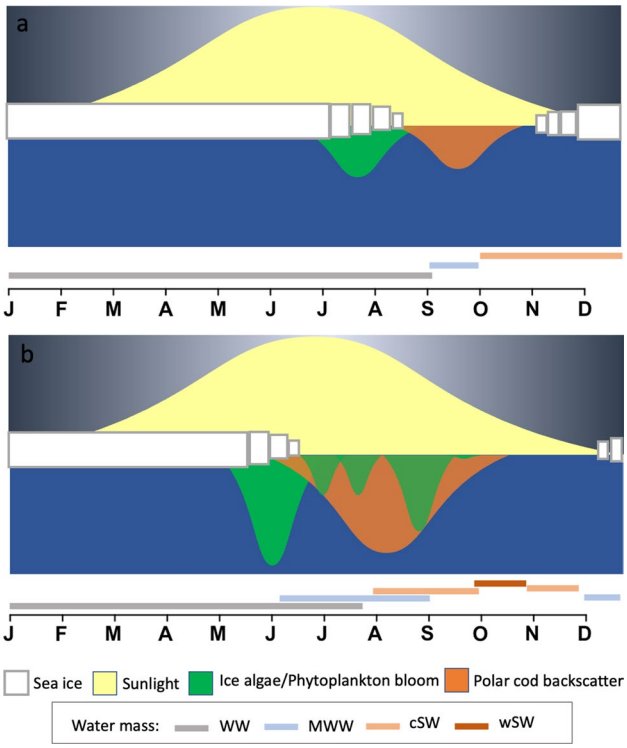

Fig. 9 Summary of temporal patterns in biological and physical variables in **a** "cold" years (2017 and 2019) and **b** "warm" years (2016 and 2018) at the Chukchi Ecosystem Observatory. *WW* Winter Water, *MWW* Modified Winter Water, *cSW* cool Shelf Water, *wSW* warm Shelf water. See Danielson et al. (2020) for water mass descriptions

growing season that leads to larger pre-winter sizes (Fortier et al. 2006; Bouchard and Fortier 2011) at the end of the growth year. Large pre-winter sizes are associated with enhanced winter survival resulting from a combination of increased lipid content, predator avoidance, resistance to starvation, and physiological tolerance (e.g. Hunt et al. 2011; Copeman et al. 2022). Later hatching when temperature, light, and food are at their maximum would result in a shorter growing season and sizes too small to ensure winter survival (Bouchard et al. 2017). It has been observed that early sea ice breakup favors higher densities of larger pre-winter polar cod (Bouchard et al. 2017). In the Canadian Arctic, the biomass of juvenile polar cod in late September was 11 times greater in a year with an early May ice breakup (< 50% ice cover) compared to a late September ice breakup (Bouchard et al. 2017). These observations are consistent with the 2–16 times greater fish densities for a May/June sea ice retreat (2017 and 2019) compared to a July sea ice retreat (2016 and 2018) observed at the CEO.

Earlier ice retreat and warmer waters enhance growth and survival of early hatchers by increasing food availability earlier in the year relative to years with late sea ice retreat (LeBlanc et al. 2019). Earlier phytoplankton blooms and extended periods of primary productivity have been observed in association with decreased sea ice in the Chukchi Sea, northern Barents Sea, and the Canadian Arctic (Zhang et al. 2015; Kahru et al. 2016; LeBlanc et al. 2019). An advanced and extended bloom results in an earlier and more intense production of copepod nauplii and copepodites (LeBlanc et al. 2019), the preferred prey of age-0 polar cod (Bouchard et al. 2016). In this study, we observed that early sea ice retreat in June 2017 was associated with earlier and extended periods of primary production and higher zooplankton densities. However, an ice retreat before June in 2019 did not result in an earlier bloom, and lower zooplankton densities were observed compared to 2017. These observations support previous studies in the Canadian Arctic (LeBlanc et al. 2019) and in the Bering Sea (Hunt et al. 2002), and suggest a potential mismatch between copepods and their food when the ice breaks earlier than June (Leu et al. 2011; Dezutter et al. 2019). Arctic copepod species such as *Calanus glacialis*, time their seasonal migration, foraging, and reproduction to ice algae and phytoplankton blooms (Leu et al. 2011). A mismatch between *C. glacialis* and its food can result in a fivefold lower biomass of *C. glacialis* in the summer that could in turn affect the recruitment of juvenile polar cod and upper trophic levels (Leu et al. 2011). This is critical to age-0 polar cod as *C. glacialis* is a key prey species (Bouchard and Fortier 2020).

Polar cod typically disperse from nursery to adult habitats at greater depths (Geoffroy et al. 2016; Forster et al. 2020), likely the Beaufort and Chukchi Slopes and Arctic Basin (Levine et al. 2021), or colonize the pack ice as age-1 fish (David et al. 2016). Observed decreased fish densities after October at the CEO could be due to a downward vertical movement of polar cod to depths below the transducer and/or to horizontal movement out of the Hanna Shoal area. In a previous study, we observed that fish targets descended to deeper waters after the summer, remained at depth until February when they started moving upwards in the water column, and reached depths closest to the surface by the end of the summer (Gonzalez et al. 2021b). These observations suggest that not all individuals may leave the area in autumn, but that some may remain at depth until February when they move upwards closer to the sea ice, in their second year of life.

TPL scaling exponents (i.e. log–log regression slopes) from this study were within the typical *b* value range of 1.5 to 2.5 (see Eisler et al. 2008) but varied among years with contrasting environmental conditions. In "warm" years, TPL slopes were significantly below the theoretical value of 2 (Taylor 1961). Kilpatrick and Ives (2003) demonstrated how negative interactions among species in a community can produce TPL slopes smaller than 2, in a fashion that may be relevant to the NE Chukchi Sea. In warmer years, enhanced northward movement of Bering Sea species, especially walleye pollock (*Gadus chalcogrammus*; Levine et al. 2021), could lead to increased interspecific competition and reductions of the TPL slope compared to "cold" years when polar cod is the dominant species (De Robertis et al. 2017). Increased abundance of age-0 polar cod in "warm" years could also increase intraspecific competition through cannibalism, a behavior previously reported for this species in the Beaufort and Chukchi Seas (Benoit et al. 2010; Gray et al. 2016) leading to reductions of the TPL slope. Observed lower fish temporal aggregation (i.e. lower temporal variability) at high fish densities in "warm" compared to "cold" years are consistent with observations reported in a previous study at the CEO (Gonzalez et al. 2021). Out-of-phase associations between water temperature and fish patchiness were observed with lowest fish and zooplankton aggregations occurring during months of highest fish and zooplankton densities (July–November).

In "cold" years, when seasonality at the CEO is more accentuated (i.e. greater temporal variability), the TPL slope was greater than the theoretical value of two. Greater slopes suggest higher temporal aggregation (i.e. greater temporal fluctuations) in polar cod densities with shorter persistence. Overall, the TPL scaling exponent *b* seems able to track changes in fish density fluctuations under different sea ice and temperature conditions in the NE Chukchi Sea. This observation is consistent with previous empirical studies suggesting that TPL exponents contain ecologically relevant information (e.g. Cobain et al. 2019; Lagrue et al. 2015; Taylor and Woiwod 1982) and can be useful ecosystem metrics (Cobain et al. 2019).

Environmental drivers of temporal patterns in polar cod backscatter

Links between oceanographic variables and fish backscatter observed in our study suggest that seasonal sea ice dynamics and water mass advection are important for the ecology of age-0 polar cod. Sea ice conditions in winter and spring have been shown to explain polar cod densities in the summer (Bouchard et al. 2017; LeBlanc et al. 2019). Via bottom-up control, the timing of sea ice retreat affects the timing, amplitude, and duration of sea ice algae and phytoplankton blooms, which stimulates and supports secondary productivity, and ultimately determines available food resources for age-0 polar cod. LeBlanc et al. (2019) observed that zooplankton backscatter in August was more strongly correlated to ice breakup date and phytoplankton bloom onset date than to chlorophyll *a* concentration, indicating that the duration of the season of food availability rather than food abundance was likely the primary driver of zooplankton biomass in late summer. In our study, significance of days after sea ice retreat, daylength, and PAR, but not of chlorophyll *a* concentration also suggest that duration of food availability rather than abundance of food might be the primary driver of secondary production, and influence age-0 polar cod growth and survival. Recruitment of age-0 polar cod provides the prey base for apex predators in subsequent years (e.g. Johnson et al. 1966; Crawford et al. 2015).

Temperature and salinity have been reported as important variables associated with polar cod abundances (De Robertis et al. 2017; Logerwell et al. 2018; Forster et al. 2020). In this study, a linear, slightly positive association between temperature (range − 2 to 4 °C) and polar cod density was observed. This trend is consistent with previous studies that report a bell-shaped association between temperature and polar cod abundances with highest abundances at 4–6 °C (Vestfals et al. 2019; Forster et al. 2020), corresponding to optimal polar cod growth temperatures (Laurel et al. 2016). Positive linear associations between polar cod density and salinities up to 34 have also been observed in previous studies (De Robertis et al. 2017; Forster et al. 2020). Temperature and salinity define water masses with characteristic nutrient concentration and phytoplankton composition (Danielson et al. 2017), which have been shown to influence the distribution of polar cod and their prey (Eisner et al. 2013). Highest polar cod densities were observed in cSW, wSW, and in MWW, which are the prevalent water masses at the CEO during spring, summer, and autumn (Danielson et al. 2020a). BCSW is often a nutrient-rich water mass (Danielson et al. 2017) with a zooplankton community composed of lipid-rich calanoid copepods and euphausiids (Eisner et al. 2013), which are prey for polar cod (Rand et al. 2013). Temporal variations in water masses influence nutrient and prey composition of the water column through time, ultimately affecting temporal patterns of polar cod densities at the CEO.

Wind patterns determine sea ice drift and water mass movement that, in turn, affect distributions of polar cod and their prey. Wind-driven variations in water flow direction have been proposed as a mechanism to explain interannual changes in age-0 gadid backscatter in the Chukchi and western Beaufort Seas (Vestfals et al. 2019; Levine et al. 2021). Flow reversals associated with strong southward winds in the summer have been used to explain the retention of polar cod in the Chukchi Shelf in the summer of 2018, whereas autumn northward winds were responsible for the northward advection of age-0 polar cod towards the Chukchi and Beaufort Shelf breaks (Levine et al. 2021).

Summary and outlook

Four years of continuous biological and physical observations at the CEO provide evidence that sea ice is a key structuring factor of the Chukchi Sea ecosystem and polar cod dynamics in particular. This study supports previous observations that earlier sea ice retreat and increases in temperature associated with enhanced water transport from the NE Pacific could temporarily benefit polar cod production in the NE Chukchi Sea. Earlier sea ice retreat results in greater and earlier peaks in polar cod densities and more stable populations (i.e. smaller fluctuations) by extending the growing season with favorable temperature and food conditions. Continuing changes in the physical environment could further alter the timing of biological processes that could lead to a mismatch of age-0 polar cod and their prey. Changes in water mass characteristics in the area could also alter the quality of polar cod prey by replacing lipid-rich species such as *C. glacialis* and *Calanus hyperboreous* by smaller, relatively lipid-poor species such as the sub-Arctic *Calanus finmarchicus* (Spear et al. 2020). Changes in zooplankton species composition and availability would likely impact polar cod growth and survival in the NE Chukchi Sea (Bouchard and Fortier 2020). Increasing temperatures and earlier transport off the Chukchi shelf due to increased northward advection of warm Pacific waters could limit age-0 growth prior to their first winter and may increase competition and predation by increasing abundances of sub-Arctic pelagic fish such as walleye pollock (Fossheim et al. 2015; Huntington et al. 2020; Levine et al. 2021). Further increases in temperatures above optimal and further loss of sea ice could also be detrimental for egg development and age-0 polar cod growth (Huserbråten et al. 2019).

As high latitudes experience increased anthropogenic and climatological pressures from fossil fuel emissions, understanding temporal patterns and environmental drivers of key Arctic ecosystem components, like polar cod, can be

used to inform resource use and management decisions. This work describes temporal patterns and environmental drivers of polar cod at the CEO during a period of unprecedented warmth and sea ice loss and provides insight into the oceanographic processes and environmental characteristics that affect polar cod feeding, growth, and survival. As similar time series become available from other parts of the Arctic, direct comparisons will be possible and will help elucidate how generic temporal patterns observed at the CEO are of patterns occurring elsewhere in the Arctic.

Supplementary Information The online version contains supplementary material available at https://doi.org/10.1007/s00300-023-03150-8.

Acknowledgements We thank the captains and crews of the M/V Norseman II, R/V Sikuliaq, R/V Ocean Starr, and USCGC Healy for CEO mooring turnarounds, along with chief scientists C. Ashjian, R. Hopcroft, K. Iken, R. McCabe, and P. Winsor. Timothy E. Essington is thanked for his valuable comments on an earlier version of the manuscript. We also thank Dr. George Divoky for constructive comments when reviewing the manuscript. SGG would like to acknowledge the support of a NPRB Graduate Student Research Award, an Oil Spill Research Institute Graduate Research Fellowship and a Fulbright-ANII Graduate Fellowship Program, and the Joint Institute for the Study of the Atmosphere and Ocean Graduate Student Award for support during her PhD Research Program. SLD acknowledges CEO support from AOOS Grants G9046 and G11133 and NPRB Projects #1426 and L36-00A (NPRB Publication # 1901). AMS acknowledges support from ANII Project FCE_3_2020_1_162710. This is the Cooperative Institute for Climate, Ocean, and Ecosystem Studies Contribution Number 2022-118.

Author contributions SG and JKH conceived and designed this study, with input from SLD. SLD provided the Chukchi Ecosystem Observatory datasets. SG processed and analyzed the data, advised by JKH, AMS, and SLD. GL analyzed the chlorophyll *a* data. SG wrote the manuscript, JKH, AMS, SLD and GL revised the manuscript.

Funding SG received support from North Pacific Research Board Graduate Student Research Award, and Oil Spill Research Institute Graduate Research Fellowship. The Chukchi Ecosystem Observatory receives operations and equipment funding from the North Pacific Research Board via Project #1426 and #19 and the Alaska Ocean Observing System via Awards #NA11NOS0120020.

Declarations

Conflict of interest The authors declare that they have no conflict of interest.

Informed consent All authors consent to the publication of this manuscript.

References

Ardyna M, Arrigo KR (2020) Phytoplankton dynamics in a changing Arctic Ocean. Nat Clim Change 10:892–903. https://doi.org/10.1038/s41558-020-0905-y

Arrigo KR, Perovich DK, Pickart RS et al (2014) Phytoplankton blooms beneath the sea ice in the Chukchi Sea. Deep Sea Res II 105:1–16. https://doi.org/10.1016/j.dsr2.2014.03.018

Arrigo KR, Perovich DK, Pickart RS et al (2012) Massive phytoplankton blooms under Arctic sea ice. Science 336:1408. https://doi.org/10.1126/science.1215065

Arrigo KR, van Dijken GL (2015) Continued increases in Arctic Ocean primary production. Prog Oceanogr 136:60–70. https://doi.org/10.1016/j.pocean.2015.05.002

Assmy P, Fernández-Méndez M, Duarte P et al (2017) Leads in Arctic pack ice enable early phytoplankton blooms below snow-covered sea ice. Sci Rep 7:1–9. https://doi.org/10.1038/srep40850

Barber WE, Smith RL, Vallarino M, Meyer RM (1997) Demersal fish assemblages of the northeastern Chukchi Sea, Alaska. Fish Bull 95:195–209

Benoit D, Simard Y, Gagné J et al (2010) From polar night to midnight sun: photoperiod, seal predation, and the diel vertical migrations of polar cod (*Boreogadus saida*) under landfast ice in the Arctic Ocean. Polar Biol 33:1505–1520. https://doi.org/10.1007/s00300-010-0840-x

Bivand R, Lewin-Koh N (2019) maptools: tools for handling spatial objects

Bluhm BA, Gradinger R (2008) Regional variability in food availability for Arctic marine mammals. Ecol Appl 18:S77–S96. https://doi.org/10.1890/06-0562.1

Bouchard C, Fortier L (2011) Circum-Arctic comparison of the hatching season of polar cod *Boreogadus saida*: a test of the freshwater winter refuge hypothesis. Prog Oceanogr 90:105–116. https://doi.org/10.1016/j.pocean.2011.02.008

Bouchard C, Fortier L (2020) The importance of *Calanus glacialis* for the feeding success of young polar cod: a circumpolar synthesis. Polar Biol. https://doi.org/10.1007/s00300-020-02643-0

Bouchard C, Geoffroy M, LeBlanc M et al (2017) Climate warming enhances polar cod recruitment, at least transiently. Prog Oceanogr 156:121–129. https://doi.org/10.1016/j.pocean.2017.06.008

Bouchard C, Mollard S, Suzuki K et al (2016) Contrasting the early life histories of sympatric Arctic gadids *Boreogadus saida* and *Arctogadus glacialis* in the Canadian Beaufort Sea. Polar Biol 39:1005–1022. https://doi.org/10.1007/s00300-014-1617-4

Cobain MRD, Brede M, Trueman CN (2019) Taylor's power law captures the effects of environmental variability on community structure: an example from fishes in the North Sea. J Anim Ecol 88:290–301. https://doi.org/10.1111/1365-2656.12923

Cohen JE, Plank MJ, Law R (2012) Taylor's law and body size in exploited marine ecosystems. Ecol Evol 2:3168–3178. https://doi.org/10.1002/ece3.418

Copeman LA, Salant CD, Stowell MA et al (2022) Annual and spatial variation in the condition and lipid storage of juvenile Chukchi Sea gadids during a recent period of environmental warming (2012 to 2019). Deep Sea Res II. https://doi.org/10.1016/j.dsr2.2022.105180

Crawford JA, Quakenbush LT, Citta JJ (2015) A comparison of ringed and bearded seal diet, condition and productivity between historical (1975–1984) and recent (2003–2012) periods in the Alaskan Bering and Chukchi Seas. Prog Oceanogr 136:133–150. https://doi.org/10.1016/j.pocean.2015.05.011

Danielson S, Ahkinga O, Ashjian C et al (2020) Manifestation and consequences of warming and altered heat fluxes over the Bering and Chukchi Sea continental shelves. Deep Sea Res II 177:104781. https://doi.org/10.1016/j.dsr2.2020.104781

Danielson SL, Eisner L, Ladd C et al (2017) A comparison between late summer 2012 and 2013 water masses, macronutrients, and phytoplankton standing crops in the northern Bering and Chukchi Seas. Deep Sea Res II 135:7–26. https://doi.org/10.1016/j.dsr2.2016.05.024

Danielson SL, Weingartner TJ, Hedstrom KS et al (2014) Coupled wind-forced controls of the Bering-Chukchi Shelf circulation and the Bering Strait throughflow: Ekman transport, continental shelf waves, and variations of the Pacific-Arctic Sea surface height

gradient. Prog Oceanogr 125:40–61. https://doi.org/10.1016/j.pocean.2014.04.006
Darnis G, Robert D, Pomerleau C et al (2012) Current state and trends in Canadian Arctic marine ecosystems: II. Heterotrophic food web, pelagic–benthic coupling, and biodiversity. Clim Change 115:179–205. https://doi.org/10.1007/s10584-012-0483-8
David C, Lange B, Krumpen T et al (2016) Under-ice distribution of polar cod *Boreogadus saida* in the central Arctic Ocean and their association with sea-ice habitat properties. Polar Biol 39:981–994. https://doi.org/10.1007/s00300-015-1774-0
De Robertis A, Taylor K, Wilson CD, Farley EV (2017) Abundance and distribution of Arctic cod (*Boreogadus saida*) and other pelagic fishes over the U.S. Continental Shelf of the Northern Bering and Chukchi Seas. Deep Sea Res II 135:51–65. https://doi.org/10.1016/j.dsr2.2016.03.002
Dezutter T, Lalande C, Dufresne C et al (2019) Mismatch between microalgae and herbivorous copepods due to the record sea ice minimum extent of 2012 and the late sea ice break-up of 2013 in the Beaufort Sea. Prog Oceanogr 173:66–77. https://doi.org/10.1016/j.pocean.2019.02.008
Divoky GJ, Lukacs PM, Druckenmiller ML (2015) Effects of recent decreases in Arctic sea ice on an ice-associated marine bird. Prog Oceanogr 136:151–161. https://doi.org/10.1016/j.pocean.2015.05.010
Drinkwater KF, Mueter FJ, Saitoh SI (2018) Shifting boundaries of water, ice, flora, fauna, people, and institutions in the Arctic and Subarctic. ICES J Mar Sci 75:2293–2298. https://doi.org/10.1093/icesjms/fsy179
Eisler Z, Bartos I, Kertész J (2008) Fluctuation scaling in complex systems: Taylor's law and beyond. Adv Phys 57:89–142. https://doi.org/10.1080/00018730801893043
Eisner L, Hillgruber N, Martinson E, Maselko J (2013) Pelagic fish and zooplankton species assemblages in relation to water mass characteristics in the northern Bering and southeast Chukchi Seas. Polar Biol 36:87–113. https://doi.org/10.1007/s00300-012-1241-0
Feurer M, Klein A, Eggensperger K et al (2015) Efficient and robust automated machine learning. In: Advances in neural information processing systems, 2015, pp 2962–2970
Forster CE, Norcross BL, Mueter FJ et al (2020) Spatial patterns, environmental correlates, and potential seasonal migration triangle of polar cod (*Boreogadus saida*) distribution in the Chukchi and Beaufort Seas. Polar Biol 43:1073–1094. https://doi.org/10.1007/s00300-020-02631-4
Fortier L, Sirois P, Michaud J, Barber D (2006) Survival of Arctic cod larvae (*Boreogadus saida*) in relation to sea ice and temperature in the Northeast Water Polynya (Greenland Sea). Can J Fish Aquat Sci 63:1608–1616. https://doi.org/10.1139/F06-064
Fossheim M, Primicerio R, Johannesen E et al (2015) Recent warming leads to a rapid borealization of fish communities in the Arctic. Nat Clim Change 5:673–677. https://doi.org/10.1038/nclimate2647
Fujiwara M, Cohen JE (2015) Mean and variance of population density and temporal Taylor's law in stochastic stage-structured density-dependent models of exploited fish populations. Theor Ecol 8:175–186. https://doi.org/10.1007/s12080-014-0242-8
Geoffroy M, Majewski A, LeBlanc M et al (2016) Vertical segregation of age-0 and age-1+ polar cod (*Boreogadus saida*) over the annual cycle in the Canadian Beaufort Sea. Polar Biol 39:1023–1037. https://doi.org/10.1007/s00300-015-1811-z
Goddard P, Lauth R, Armistead C (2014) Results of the 2012 Chukchi Sea bottom trawl survey of bottomfishes, crabs, and other demersal macrofauna. U.S. Department Commerce, NOAA Technical Memorandum, NMFS-AFSC-278, Seattle
Gonzalez S, Horne JK, Danielson SL (2021) Multi-scale temporal variability in biological–physical associations in the NE Chukchi Sea. Polar Biol. https://doi.org/10.1007/s00300-021-02844-1
Gradinger R (2009) Sea-ice algae: major contributors to primary production and algal biomass in the Chukchi and Beaufort Seas during May/June 2002. Deep Sea Res II 56:1201–1212. https://doi.org/10.1016/j.dsr2.2008.10.016
Graham M, Hop H (1995) Aspects of reproduction and larval biology of Arctic cod (*Boreogadus saida*). Arct Inst N Am 48:130–135
Gray BP, Norcross BL, Blanchard AL et al (2016) Variability in the summer diets of juvenile polar cod (*Boreogadus saida*) in the northeastern Chukchi and western Beaufort Seas. Polar Biol 39:1069–1080. https://doi.org/10.1007/s00300-015-1796-7
Grebmeier JM (2012) Shifting patterns of life in the Pacific Arctic and sub-Arctic Seas. Annu Rev Mar Sci 4:63–78. https://doi.org/10.1146/annurev-marine-120710-100926
Grebmeier JM, Bluhm BA, Cooper LW et al (2015) Ecosystem characteristics and processes facilitating persistent macrobenthic biomass hotspots and associated benthivory in the Pacific Arctic. Prog Oceanogr 136:92–114. https://doi.org/10.1016/j.pocean.2015.05.006
Hannay DE, Delarue J, Mouy X et al (2013) Marine mammal acoustic detections in the northeastern Chukchi Sea, September 2007–July 2011. Cont Shelf Res 67:127–146. https://doi.org/10.1016/j.csr.2013.07.009
Harwood LA, Smith TG, George JC et al (2015) Change in the Beaufort Sea ecosystem: diverging trends in body condition and/or production in five marine vertebrate species. Prog Oceanogr 136:263–273. https://doi.org/10.1016/j.pocean.2015.05.003
Hastie T, Tibshirani R (1990) Generalized additive models. Chapman and Hall, London
Hersbach H, Bell B, Berrisford P et al (2018) ERA5 hourly data on single levels from 1979 to present. Copernicus Climate Change Service (C3S) Climate Data Store (CDS)
Hill V, Ardyna M, Lee SH, Varela DE (2018a) Decadal trends in phytoplankton production in the Pacific Arctic Region from 1950 to 2012. Deep Sea Res II 152:82–94. https://doi.org/10.1016/j.dsr2.2016.12.015
Hill VJ, Light B, Steele M, Zimmerman RC (2018b) Light availability and phytoplankton growth beneath Arctic sea ice: Integrating observations and modeling. J Geophys Res Ocean 123:3651–3667. https://doi.org/10.1029/2017JC013617
Hop H, Falk-Petersen S, Svendsen H et al (2006) Physical and biological characteristics of the pelagic system across Fram Strait to Kongsfjorden. Prog Oceanogr 71:182–231. https://doi.org/10.1016/j.pocean.2006.09.007
Hunt GL, Coyle KO, Eisner LB et al (2011) Climate impacts on eastern Bering Sea foodwebs: a synthesis of new data and an assessment of the Oscillating Control Hypothesis. ICES J Mar Sci 68:1230–1243. https://doi.org/10.1093/icesjms/fsr036
Hunt GL, Stabeno P, Walters G et al (2002) Climate change and control of the southeastern Bering Sea pelagic ecosystem. Deep Sea Res II 49:5821–5853. https://doi.org/10.1016/S0967-0645(02)00321-1
Huntington HP, Danielson SL, Wiese FK et al (2020) Evidence suggests potential transformation of the Pacific Arctic ecosystem is underway. Nat Clim Change. https://doi.org/10.1038/s41558-020-0695-2
Huserbråten MBO, Eriksen E, Gjøsæter H, Vikebø F (2019) Polar cod in jeopardy under the retreating Arctic sea ice. Commun Biol 2:1–8. https://doi.org/10.1038/s42003-019-0649-2
Jay CV, Fischbach AS, Kochnev AA (2012) Walrus areas of use in the Chukchi Sea during sparse sea ice cover. Mar Ecol Prog Ser 468:1–13. https://doi.org/10.3354/meps10057

Ji R, Jin M, Varpe Ø (2013) Sea ice phenology and timing of primary production pulses in the Arctic Ocean. Glob Change Biol 19:734–741. https://doi.org/10.1111/gcb.12074

Johnson ML, Fiscus CH, Ostenson BT, Barbour ML (1966) Marine mammals. In: Wilimovsky NJ, Wolfe JN (eds) Environment of the Cape Thompson Region, Alaska. U.S. Atomic Energy Commission, Oak Ridge, pp 897–924

Kahru M, Lee Z, Mitchell BG, Nevison CD (2016) Effects of sea ice cover on satellite-detected primary production in the Arctic Ocean. Biol Lett 12:20160223. https://doi.org/10.1098/rsbl.2016.0223

Kang M, Furusawa M, Miyashita K (2002) Effective and accurate use of difference in mean volume backscattering strength to identify fish and plankton. ICES J Mar Sci 59:794–804. https://doi.org/10.1006/jmsc.2002.1229

Kilpatrick AM, Ives AR (2003) Species interactions can explain Taylor's power law for ecological time series. Nature 422:65–68. https://doi.org/10.1038/nature01471

Kono Y, Sasaki H, Kurihara Y et al (2016) Distribution pattern of Polar cod (*Boreogadus saida*) larvae and larval fish assemblages in relation to oceanographic parameters in the northern Bering Sea and Chukchi Sea. Polar Biol 39:1039–1048. https://doi.org/10.1007/s00300-016-1961-7

Korneliussen RJ, Ona E (2003) Synthetic echograms generated from the relative frequency response. ICES J Mar Sci 60:636–640. https://doi.org/10.1016/S1054-3139(03)00035-3

Kuo TC, Mandal S, Yamauchi A, Hsieh CH (2016) Life history traits and exploitation affect the spatial mean–variance relationship in fish abundance. Ecology 97:1251–1259. https://doi.org/10.1890/15-1270.1/suppinfo

Kwok R (2018) Arctic sea ice thickness, volume, and multiyear ice coverage: losses and coupled variability (1958–2018). Environ Res Lett. https://doi.org/10.1088/1748-9326/aae3ec

Lagrue C, Poulin R, Cohen JE (2015) Parasitism alters three power laws of scaling in a metazoan community: Taylor's law, density-mass allometry, and variance-mass allometry. Proc Natl Acad Sci USA 112:1791–1796. https://doi.org/10.1073/pnas.1422475112

Laurel BJ, Spencer M, Iseri P, Copeman LA (2016) Temperature-dependent growth and behavior of juvenile Arctic cod (*Boreogadus saida*) and co-occurring North Pacific gadids. Polar Biol 39:1127–1135. https://doi.org/10.1007/s00300-015-1761-5

LeBlanc M, Geoffroy M, Bouchard C et al (2019) Pelagic production and the recruitment of juvenile polar cod *Boreogadus saida* in Canadian Arctic seas. Polar Biol. https://doi.org/10.1007/s00300-019-02565-6

Leu E, Søreide JE, Hessen DO et al (2011) Consequences of changing sea-ice cover for primary and secondary producers in the European Arctic shelf seas: timing, quantity, and quality. Prog Oceanogr 90:18–32. https://doi.org/10.1016/j.pocean.2011.02.004

Levine RM, De Robertis A, Grünbaum D et al (2021) Autonomous vehicle surveys indicate that flow reversals retain juvenile fishes in a highly advective high-latitude ecosystem. Limnol Oceanogr 66:1139–1154. https://doi.org/10.1002/lno.11671

Lewis KM, Van Dijken GL, Arrigo KR (2020) Changes in phytoplankton concentration now drive increased Arctic Ocean primary production. Science 369:198–202

Li WKW, McLaughlin FA, Lovejoy C, Carmack EC (2009) Smallest algae thrive as the Arctic Ocean freshens. Science 326:539. https://doi.org/10.1126/science.1179798

Logerwell E, Rand K, Danielson S, Sousa L (2018) Environmental drivers of benthic fish distribution in and around Barrow Canyon in the northeastern Chukchi Sea and western Beaufort Sea. Deep Sea Res II 152:170–181. https://doi.org/10.1016/j.dsr2.2017.04.012

Lowry LF, Frost KJ (1981) Distribution, growth, and foods of Arctic cod (*Boreogadus saida*) in the Bering, Chukchi and Beaufort Seas. Can Field Nat 95:186–191

Madureira LSP, Ward P, Atkinson A (1993) Differences in backscattering strength determined at 120 and 38 kHz for three species of Antarctic macroplankton. Mar Ecol Prog Ser 93:17–24. https://doi.org/10.3354/meps093017

Marsh JM, Mueter FJ (2019) Influences of temperature, predators, and competitors on polar cod (*Boreogadus saida*) at the southern margin of their distribution. Polar Biol. https://doi.org/10.1007/s00300-019-02575-4

Maslanik J, Stroeve J (1999) Near-Real-Time DMSP SSMIS Daily Polar Gridded Sea Ice Concentrations, Version 1. In: Boulder, Color. USA. NASA Natl. Snow Ice Data Cent. Distrib. Act. Arch. Cent.

Maurer BA (1999) Untangling ecological complexity: the macroscopic perspective. University of Chicago Press, Chicago

Mellin C, Huchery C, Caley MJ et al (2010) Reef size and isolation determine the temporal stability of coral reef populations. Ecology 91:3138–3145

Møller EF, Nielsen TG (2019) Borealization of Arctic zooplankton—smaller and less fat zooplankton species in Disko Bay, Western Greenland. Limnol Oceanogr. https://doi.org/10.1002/lno.11380

Mueter F, Bouchard C, Hop H et al (2020) Arctic gadids in a rapidly changing environment. Polar Biol. https://doi.org/10.1007/s00300-020-02696-1

Mundy CJ, Barber DG, Michel C (2005) Variability of snow and ice thermal, physical and optical properties pertinent to sea ice algae biomass during spring. J Mar Syst 58:107–120. https://doi.org/10.1016/j.jmarsys.2005.07.003

NPFMC (2009) Fishery Management Plan for Fish Resources of the Arctic Management Area. NPFMC

Polyakov IV, Alkire MB, Bluhm BA et al (2020) Borealization of the Arctic Ocean in response to anomalous advection from sub-Arctic Seas. Front Mar Sci. https://doi.org/10.3389/fmars.2020.00491

Post E, Bhatt US, Bitz CM et al (2013) Ecological consequences of sea-ice decline. Science 341:519–524. https://doi.org/10.1126/science.1235225

Rand KM, Whitehouse A, Logerwell EA et al (2013) The diets of polar cod (*Boreogadus saida*) from August 2008 in the US Beaufort Sea. Polar Biol 36:907–912. https://doi.org/10.1007/s00300-013-1303-y

Segura A, Wiff R, Jaureguizar AJ et al (2021) A macroecological perspective on the fluctuations of exploited fish populations. Mar Ecol Prog Ser 665:177–183. https://doi.org/10.3354/meps13662

Serreze MC, Barrett AP, Crawford AD, Woodgate RA (2019) Monthly variability in Bering Strait oceanic volume and heat transports, links to atmospheric circulation and ocean temperature, and implications for sea ice conditions. J Geophys Res Ocean 124:9317–9337. https://doi.org/10.1029/2019JC015422

Serreze MC, Crawford AD, Stroeve JC et al (2016) Variability, trends, and predictability of seasonal sea ice retreat and advance in the Chukchi Sea. J Geophys Res Ocean 121:7308–7325. https://doi.org/10.1002/2016JC011977

Sigler MF, Mueter FJ, Bluhm BA et al (2017) Late summer zoogeography of the northern Bering and Chukchi Seas. Deep Sea Res II 135:168–189. https://doi.org/10.1016/j.dsr2.2016.03.005

Sigler MF, Rooper CN, Hoff GR et al (2015) Faunal features of submarine canyons on the eastern Bering Sea slope. Mar Ecol Prog Ser 526:21–40. https://doi.org/10.3354/meps11201

Søreide JE, Leu EVA, Berge J et al (2010) Timing of blooms, algal food quality and *Calanus glacialis* reproduction and growth in a changing Arctic. Glob Change Biol 16:3154–3163. https://doi.org/10.1111/j.1365-2486.2010.02175.x

Spear A, Napp J, Ferm N, Kimmel D (2020) Advection and in situ processes as drivers of change for the abundance of large zooplankton taxa in the Chukchi Sea. Deep Sea Res II 177:104814. https://doi.org/10.1016/j.dsr2.2020.104814

Steele M, Ermold W, Zhang J (2008) Arctic Ocean surface warming trends over the past 100 years. Geophys Res Lett 35:1–6. https://doi.org/10.1029/2007GL031651

Stroeve J, Notz D (2018) Changing state of Arctic sea ice across all seasons. Environ Res Lett. https://doi.org/10.1088/1748-9326/aade56

Taylor LR (1961) Aggregation, variance and the mean. Nature 189:732–735

Taylor LR, Woiwod IP (1982) Comparative synoptic dynamics. I. Relationships between inter- and intra-specific spatial and temporal variance/mean population parameters. Br Ecol Soc 51:879–906

Timmermans ML, Labe Z (2020) Sea surface temperature. NOAA Arct Rep Card. https://doi.org/10.25923/v0fs-m920

Vestfals CD, Mueter FJ, Duffy-Anderson JT et al (2019) Spatio-temporal distribution of polar cod (*Boreogadus saida*) and saffron cod (*Eleginus gracilis*) early life stages in the Pacific Arctic. Polar Biol 42:969–990. https://doi.org/10.1007/s00300-019-02494-4

Weingartner T, Aagaard K, Woodgate R et al (2005a) Circulation on the north central Chukchi Sea shelf. Deep Sea Res II 52:3150–3174. https://doi.org/10.1016/j.dsr2.2005.10.015

Weingartner T, Aagaard K, Woodgate R, Danielson S (2005b) Circulation on the north central Chukchi Sea shelf. Deep Sea Res II 52:3150–3174. https://doi.org/10.1016/j.dsr2.2005.10.015

Welch HE, Bergmann MA, Siferd TD et al (1992) Energy flow through the marine ecosystem of the Lancaster Sound Region, Arctic Canada. Arct Inst N Am 45:343–357

Whitehouse GA, Aydin K, Essington TE, Hunt GL (2014) A trophic mass balance model of the eastern Chukchi Sea with comparisons to other high-latitude systems. Polar Biol 37:911–939. https://doi.org/10.1007/s00300-014-1490-1

Wood S (2004) Stable and efficient multiple smoothing parameter estimation for Generalized Additive Models. J Am Stat Assoc 99:673–686. https://doi.org/10.1198/016214504000000980

Wood S (2017) Generalized additive models: an introduction with R, 2nd edn. Chapman and Hall/CRC Press, Boca Raton

Wood S (2011) Fast stable restricted maximum likelihood and marginal likelihood estimation of semiparametric generalized linear models. J R Stat Soc B 73:3–36. https://doi.org/10.1111/j.1467-9868.2010.00749.x

Woodgate RA, Aagaard K, Weingartner TJ (2005) Monthly temperature, salinity, and transport variability of the Bering Strait through flow. Geophys Res Lett 32:1–4. https://doi.org/10.1029/2004GL021880

Woodgate RA, Peralta-Ferriz C (2021) Warming and freshening of the Pacific inflow to the Arctic from 1990–2019 implying dramatic shoaling in Pacific Winter Water ventilation of the Arctic water column. Geophys Res Lett 48:1–11. https://doi.org/10.1029/2021GL092528

Wu Z, Wang X (2018) Variability of Arctic sea ice (1979–2016). Water 11:1–10. https://doi.org/10.3390/w11010023

Zhang J, Ashjian C, Campbell R et al (2015) The influence of sea ice and snow cover and nutrient availability on the formation of massive under-ice phytoplankton blooms in the Chukchi Sea. Deep Sea Res II 118:122–135. https://doi.org/10.1016/j.dsr2.2015.02.008

Zuur AF, Ieno EN, Walker NJ et al (2009) Mixed effects models and extensions in ecology with R. Springer, New York